Nuclear Instruments and Methods in Physics Research B 490 (2021) 39–42

Contents lists available at ScienceDirect

Nuclear Inst. and Methods in Physics Research, B

journal homepage: www.elsevier.com/locate/nimb

Deep levels in ion implanted n-type homoepitaxial GaN: Ion mass, tilt angle and dose dependence

G. Alfieri [a,*], V.K. Sundaramoorthy [a], R. Micheletto [b]

[a] Hitachi-ABB Power Grids, Fabrikstrasse 3, 5600 Lenzburg, Switzerland
[b] Department of Materials System Science, Yokohama City University, Yokohama 236-0027, Japan

ARTICLE INFO

Keywords:
GaN
Ion implantation
Deep levels
DLTS

ABSTRACT

Ion implantation is a fundamental processing step in electronic device manufacturing. However, it can give rise to electrically active defects, in the crystal, that can undermine the functionality of devices. In this study, we carried out an electrical characterization study of defects in ion implanted n-type GaN. We found several levels in the 0.2–1.2 eV below the conduction band edge. The nature of these defects is discussed in the light of the ion mass, tilt angle and dose dependence of the concentration of the detected levels.

1. Introduction

Ion implantation (I/I) is a faster and cheaper alternative to growth for selective area doping in semiconductor device manufacturing, for forming anodes (cathodes) or junction termination extensions (JTE). These structures rely on the formation of an implantation box-profile, that is the implant of a selected ion (typically p- or n-type dopant species) with multiple energies and high total doses ($> 10^{11}$ cm^{-2}) [1,2].

If on one hand growth could lead to the introduction of unwanted impurities, on the other I/I at high doses leads to amorphization and to the formation of point defects in the implant tail region [1], that is the part of the implantation profile that is located deeper in the epilayer. Amorphization can be avoided by performing high-temperature I/I, but this does not prevent the formation of electrically active levels in the band gap which are detrimental for electronic device operation [1].

While the issue of implantation induced electrically active point defects in 4H-SiC has been studied in detail in the past, this topic has not been thoroughly investigated in GaN. For instance, it is known that most of the implantation induced defects in 4H-SiC anneal out at temperatures below 1300 °C [3,4] and V_C [5], carbon interstitial (C_i) or silicon related defects [4,6] have been identified. In the case of GaN, it was recently shown that several electrically active levels, in the 0.2–1.2 eV energy range, below the conduction band edge (E_C), are present in the implant tail region and many of these survive annealing temperatures of at least 1000 °C with concentrations in the 10^{14} –10^{16} cm^{-3} range [7]. The nature of I/I induced defects in GaN is not known, yet. The reason is that GaN surface can easily decompose for heat treatments above 1000 °C, unless special conditions are employed [2]. This makes annealing studies, which can give information on the microscopic structure of defects, complicated to carry out in GaN.

To overcome this limitation, an alternative is to study the presence of electrical active defects as a function of I/I parameters. To do this, we carried out the electrical characterization of defects in implanted homoepitaxial GaN, as a function of the I/I ion mass, tilt angle and dose.

2. Experimental details

We employed 1 μm thick Si-doped n-type GaN epilayers (net donor concentration, N_d, 3–5 × 10^{16} cm^{-3}, [C]∼1–3×10^{16} cm^{-3}). Epilayers, purchased from NTT (Japan), were grown by metallorganic chemical vapor deposition (MOCVD) on highly doped GaN hydride vapor phase epitaxy (HVPE) substrates. Different sets of samples were prepared for I/I of:

- 70 keV beryllium (9.01 a.m.u., dose 10^{11} cm^{-2})
- 150 keV carbon (12.01 a.m.u., doses 4 × 10^{11} cm^{-2}, 4 × 10^{11} cm^{-2} or 4 × 10^{12} cm^{-2})
- 150 keV oxygen (15.99 a.m.u., dose 10^{11} cm^{-2})
- 250 keV manganese (54.93 a.m.u., dose 10^{11} cm^{-2})
- 250 keV indium (114.82 a.m.u., dose 10^{11} cm^{-2})

All I/I were performed with 0° tilt (channeled I/I), except in the case of In for which also random (10°) I/I was carried out. I/I energies were chosen by Monte Carlo full collision cascades simulations (SRIM) [8] so

* Corresponding author.
E-mail address: giovanni.alfieri@hitachi-powergrids.com (G. Alfieri).

https://doi.org/10.1016/j.nimb.2020.12.010
Received 6 October 2020; Received in revised form 15 December 2020; Accepted 16 December 2020
Available online 22 January 2021
0168-583X/

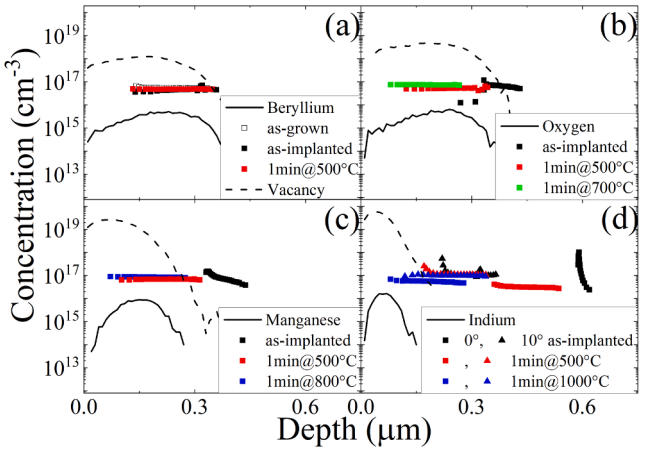

Fig. 1. Ion implantation and total vacancies profile simulated by SRIM [8], compared to the N_d concentration behavior, measured by C-V after I/I and annealing at different temperatures, for (a) Be, (b) O, (c) Mn and (d) In 0° I/I. For (d), square symbols are related to I/I at 0° tilt, whereas triangles are for 10° tilt.

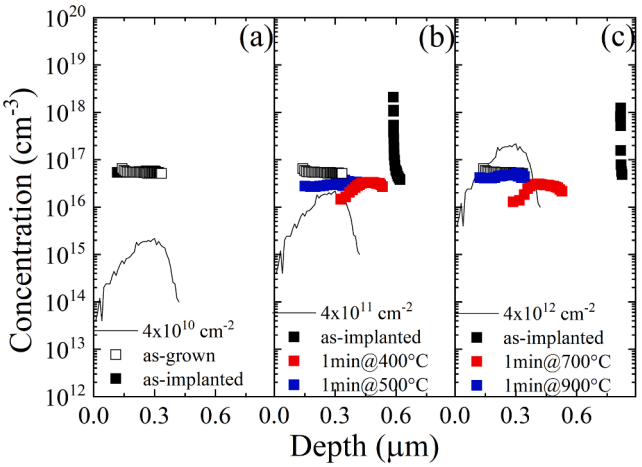

Fig. 2. Simulated C I/I profile and behavior of N_d, at different annealing temperatures, for dose values of (a) 4×10^{10} cm^2, (b) 4×10^{11} cm^2 and (c) 4×10^{12} cm^2.

to have an implantation profile maximum located at ~0.15–0.25 μm. Doses were chosen in order to simulate the tail region of an implant box-profile.

After implantation, samples were cleaned in a mixture of H_2O:HCl and then 70 nm Ni was deposited on the epilayer through a shadow mask (1 mm diameter), while Ag paste was employed as ohmic contacts, on the substrate. Electrical characterization was carried out by C-V at room-temperature and Fourier-transform deep level transient spectroscopy (DLTS) measurements [9], in the 100–650 K range. For DLTS, the reverse bias was set to −6 V, on order to cover the implantation profile, and the pulse voltage was set to 6 V for 1 ms.

All samples underwent annealing at 800 and 1000 °C, for 1 min, in Ar ambient, using a rapid thermal annealing (RTA) furnace. Prior to heat treatments, Ag paste was removed by acetone and metal contacts by aqua regia.

3. Results and discussion

3.1. N_d concentration profiles

In fig. 1 we show the results of our Monte Carlo simulations [8] against N_d measured by C-V. All implantations were carried out at 0° (channeled). For the In case, we compare the 0° to the 10° tilted I/I. In the figure, the results of samples annealed at 500 and 700, 800 and 1000 °C are also shown. This was done to evaluate the level of N_d compensation (or loss of charge carriers) of various species. In each graph the solid and dashed curves represent the simulation results of the I/I and total vacancies profile, respectively. The colored geometrical symbols represent the measurement done with C-V method. As the figure shows, the N_d profile does not change with respect to the as-grown GaN levels, after Be implantation (fig. 1(a)). After O (and C, 4×10^{11} cm^2) implantation, N_d compensation is observed in the implanted area and this is relieved after annealing at 500 °C (fig. 1(b)). A similar effect is found also after Mn implantation(fig. 1(c)), whereas, in the case of the heaviest ion employed in this study (In), heat treatments of above 1000 °C might be needed to achieve complete N_d reactivation in the implanted area (fig. 1(d), square symbols). The overshoot of N_d, compared to the as-grown values, occurs due to compensation and to the presence of a non-uniform density of traps [10].

The reason of the behavior of N_d can be found in the density of the collision cascades: the larger the mass, the higher the density of the collision cascades. Typically, in a low density collision cascade, Frenkel pairs (vacancies and interstitials) can recombine more efficiently [11,12]. This does not occur for denser cascades in which, electrically active complex defects or clusters might form leading to compensation. As Uedono et al. [13] have reported, I/I in GaN leads to the formation of Ga and N vacancies, V_{Ga} and V_N, respectively, and their complexes. In the case of O (C) and Mn, heat treatments at ~ 500 °C are sufficient for N_d reactivation. Interestingly, this is about the same temperature at which the annealing of Ga interstitials (Ga_i) and V_{Ga} occurs [14]. Although the total vacancy concentration with respect to the Mn case (fig. 1(c)) is similar, the reason for the higher annealing temperature required for the In case might be found in the presence of defects that form electrically inactive defect complexes with Si doping (doping passivation) [15].

In order to investigate the N_d behavior as a function of the I/I tilt, we compare the cases of In I/I with 0° and 10° tilt. The results are shown in fig. 1(d) where square symbols represent 0° and triangle symbols the 10° tilt. Unlike the 0° tilt case, after I/I with 10°, N_d is detected in a region close to the implanted In (~ 0.3μm). The reason for this is that channeled I/I can display a deep implant tail, whereas tilted I/I does not [16,17]. Yet, in either channeled or tilted I/I, defects (primary or higher order ones) forming at the implant tail are responsible for the compensation (or passivation) of N_d. In addition, subsequent heat treatments up to 1000 °C do not result in the full reactivation of N_d in the implanted area, like the 0° case. This suggests that defects of very similar nature form in both channeled and tilted I/I.

For the N_d behavior dependence on the I/I dose, we consider the case of C (0° tilt). As fig. 2 shows, the lowest dose case (4×10^{10} cm^2) is similar to that of Be I/I, with neither passivation nor compensation taking place. The situation changes for a dose of 4×10^{11} cm^2, for which implantation leads to compensation in the implanted region. N_d recovers after annealing at 500 °C, indicating the presence of V_{Ga} or Ga_i-related defects, as mentioned above. The highest dose 4×10^{12} cm^2 implantation resembles the afore mentioned In implantation case (fig. 1(d), square symbols), with the difference that slightly lower annealing temperature (900 °C) is required to achieve reactivation in the implanted area. Since a significant C content is present in the MOCVD grown epilayers employed in this study, we cannot rule out doping passivation is not only caused by vacancies but also by C, such as the case of the neutral complexes $Si_{Ga}C_N$ and $Si_{Ga}C_i$ [15]. This might also apply to the In case (fig. 1(d)).

3.2. Deep levels characterization

In fig. 3, we show the results of the DLTS characterization performed on the 800 °C and 1000 °C implanted and annealed GaN epilayers. In the

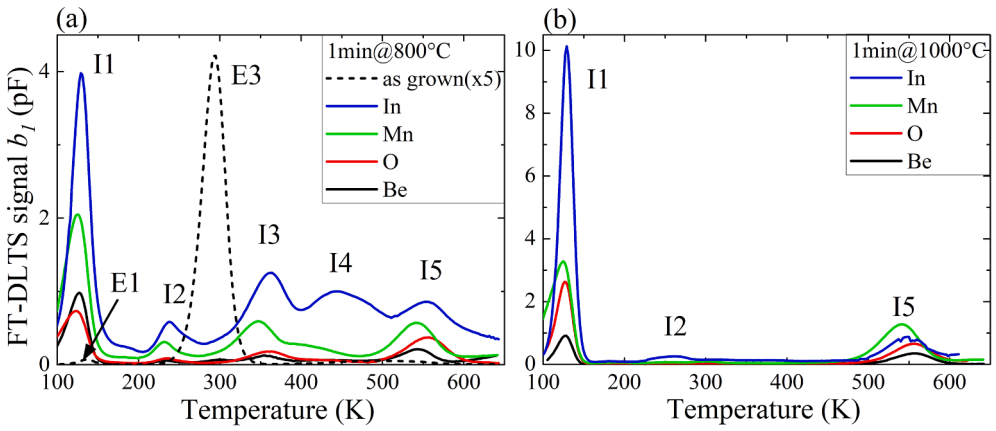

Fig. 3. DLTS spectra of n-type GaN implanted with Be, O, Mn and In after (a) 800 °C and (b) 1000 °C. Dashed line represent the spectrum of as-grown n-type GaN. The period width is 0.2 s.

as grown samples we find two electrically active levels, known as E1 and E3 at 0.2 and 0.56 eV below the conduction band edge (E_C), respectively. E1 and E3 have a concentration of 10^{13}cm^{-3} and 10^{14}cm^{-3}, respectively. After implantation and annealing at 800 °C, we detect five electrically active levels. These have been labeled I1, I2, I3, I4 and I5 and, from the Arrhenius plot dependence of the emission rates, we find that they are located at E_C-0.2 eV, E_C-0.42 eV, E_C-0.7 eV, E_C-0.82 eV, E_C-1.2 eV, respectively. Of these, only three levels survive heat treatments at 1000 °C. A slight shift in the DLTS peak position of I2, I3 and I5 can be observed for larger ion masses, which can be attributed to the higher crystal strain caused by implantation or to the formation of minor contribution that tend to smear out the DLTS peaks.

The plot of the concentrations of the detected levels versus the ion mass is shown in fig. 4. It can be observed that the concentration of all levels increases with increasing ion mass. Such effect was observed also in Si [18]. This, together to the high thermal stability [19], can be an indication of the complex nature of the detected centers. In addition, as the heavier the ion, the larger the collision cascades [20], it can be thought that in denser collision cascade the probability of complex formation is higher due a less efficient recombination of V_N (V_{Ga}) with nitrogen (gallium) interstitials N_i (Ga_i).

By varying the I/I tilt angle, no difference in the presence of the detected levels was observed. However, their concentration is strongly dependent on the tilt angle, as a higher concentration is found for the channeled I/I than for the 10° one (see black symbols in fig. 4). Although it was reported that a higher concentration of defects is expected for tilted I/I, the present finding is not unusual. Deenaparay et al. [21] have reported that, unlike P I/I, He implantation of Si shows no clear I/I angle dependence of the concentration, as the concentration of some levels can decrease for increasing tilt. According to our Monte Carlo simulations, no difference in the total vacancies concentration and distribution is observed, for channeled and tilted I/I. For this reason, it can be thought that a major role in the nature of the detected levels is played by Ga_i, which are known to be mobile even at room temperature [14]. The reason for the higher concentration can be found in the fact that Ga_i is more stable in the center of the hexagonal channel [22]. Clearly, this position might be easier to achieve via a channeled I/I rather than in the tilted one.

The dose dependence is shown in Fig. 5. This shows a sublinear or close to linear dose dependence for all the detected levels, indicating the occurrence of intercascade point defect recombination [23]. This excludes the possibility higher order complexes formation, e.g. clusters of intrisic defects, while we speculate that the detected levels might arise from the interaction of intrinsic defects, e.g. Ga_i, existing in different collision cascades.

As our results show, the levels reported in this study are found irrespective of the projectile type. This suggests the fact that implanted species have no role in the microscopic structure of the generated defects. It can be then assumed that, after ion implantation, defects forming at the implant tail region of a box-profile are of intrinsic nature, e.g. complexes of intrinsic defects, or complexes related to impurities incorporated during growth, such as Si, O, C or Fe [24].

The I1 level, which is also present in the as-grown samples, is identified as the E1 and has been associated to the divacancy (V_NV_{Ga}) [25]. The other level found in the as-grown material (E3) is not noticeable

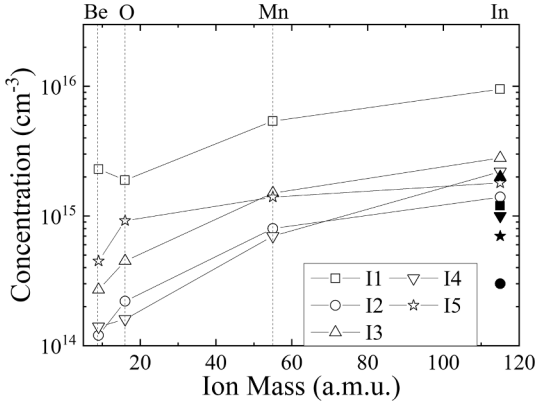

Fig. 4. Concentrations of the I1, I2, I3, I4 and I5 levels as a function of the implanted ion mass. White symbols refer to channeled implantation, black ones to tilted implantation.

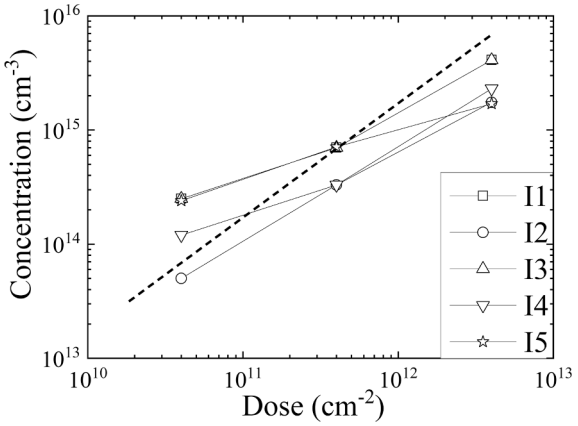

Fig. 5. Concentrations of the I1, I2, I3, I4 and I5 levels as a function of the C implantation dose.

Table 1
Energy position in the band gap, capture cross section and possible origin of the centers found in the present study.

Label	Energy position (eV)	Capture cross section (cm^2)	Possible origin
E1	E_C-0.2	3.3×10^{-17}	divacancy, same as I1
E3	E_C-0.56	7.2×10^{-16}	Fe impurity
I2	E_C-0.42	4.1×10^{-14}	C-related complex?
I3	E_C-0.70	3.0×10^{-16}	interstitial related
I4	E_C-0.82	1.5×10^{-16}	intrinsic complex defect?
I5	E_C-1.2	3.6×10^{-15}	intrinsic complex defect?

after implantation and annealing. After Be implantation a very small peak can be observed at ∼ 300 K, but no such signal is present in O, Mn or In implantation, even after 1000°C annealing. Since the E3 level was associated to Fe-impurity [26], it can be thought that implantation causes the substitutional Fe (Fe_{Ga}) to be knocked off from its position.

The I2 level was also found in Mg-implanted samples and labeled M6. Its microscopic structure was associated to a C-related complex. As a matter of fact, it was found that the activation energy for the annealing of M6 [7] was close to the energy barrier of C-diffusion in n-type GaN.

The I3 DLTS peak was also reported in Mg-implanted n-type [7] and labelled M3. This level is similar to the one found both in N-implanted [27] and Eu implanted [28] material and associated to nitrogen interstitials (N_i). The I4 DLTS peak has also quite broad features, suggesting that it can also be due to the overlapping of minor contributions. This was also found in electron irradiated n-type GaN [29], but no hypothesis have been put forward on its nature. The nature of the deepest level found in this study, I5, is also not known. However, C-implantation studies have shown that its nature may not be related to C [30].

A summary of the detected levels, their energy position in the band gap, capture cross section and a comment on their possible microscopic structure, is reported in Table 1.

4. Conclusions

We carried out the electrical characterization of ion implanted n-type GaN and found five electrically active levels in the 0.2–1.2 eV energy range below E_C. The nature of these levels was studied as a function of the projectile mass, implantation tilt angle and dose. It is found that the detected levels can be associated to intrinsic defects or complexes with intrinsic impurities, e.g. Si.

Declaration of Competing Interest

The authors declare that they have no known competing financial interests or personal relationships that could have appeared to influence the work reported in this paper.

References

[1] T. Kimoto, J.A. Cooper, Fundamentals of Silicon Carbide technology, Wiley, Singapore, 2014.
[2] T. Narita, H. Yoshida, K. Tomita, K. Kataoka, H. Sakurai, M. Horita, M. Bockowski, N. Ikarashi, J. Suda, T. kachi, Y. Tokuda, J. Appl. Phys. 128, 090901 (2020).
[3] G. Alfieri, E.V. Monakhov, B.G. Svensson, M.K. Linnarsson, J. Appl. Phys. 98 (2005), 043518.
[4] G. Alfieri, A. Mihaila, J. Phys.: Condens. Matter 32 (2020), 465703.
[5] N.T. Son, X.T. Trinh, L.S. Lovlie, B.G. Svensson, K. Kawahara, J. Suda, T. Kimoto, T. Umeda, J. Isoya, T. Makino, T. Ohshima, E. Janzen, Phys. Rev. Lett. 109 (2012), 187603.
[6] M.L. David, G. Alfieri, E.V. Monakhov, A. Hallen, C. Blanchard, B.G. Svensson, J. F. Barbot, J. Appl. Phys. 95 (2004) 4728.
[7] G. Alfieri, V.K. Sundaramoorthy, R. Micheletto, J. Appl. Phys. 123 (2018), 205303.
[8] J.F. Ziegler, et al., The Stopping and Range of Ions in Solids, Pergamon, New York, 1985.
[9] S. Weiss, R. Kassing, Solid-State Electron. 31 (1988) 1733.
[10] D. Åberg, A. Hallen, B.G. Svensson, Physica B273–274 (1999) 672.
[11] E. Wendler, B. Breeger, C. Schubert, W. Wesch, Nucl. Instr. Meth. Phys. Res. B 147 (1999) 155.
[12] S.O. Kucheyev, J.S. Williams, A.I. Titov, G. Li, C. Jagadish, Appl. Phys. Lett. 78 (2001) 2694.
[13] A. Uedono, K. Ito, H. Nakamori, K. Mori, Y. Nakano, T. Kachi, S. Ishibashi, T. Ohdaira, R. Suzuki, J. Appl. Phys. 102 (2007), 084505.
[14] F. Tuomisto, V. Ranki, D.C. Look, G.C. Farlow, Phys. Rev. B 76 (2007), 165207.
[15] M. Matsubara, E. Bellotti, J. Appl. Phys. 121 (2017), 195702.
[16] J. Wong-Leung, M.S. Janson, A. Kuznetsov, B.G. Svensson, M.K. Linnarsson, A. Hallen, C. Jagadish, D.J.H. Cockayne, Nucl. Instr. Meth. Phys. Res. B 266 (2008) 1367.
[17] F.R. Ding, A. Vantomme, W.H. He, Q. Zhao, B. Pipeleers, K. Jacobs, I. Moerman, K. Iakoubovskii, G.J. Adriaenssens, Mat. Sci. Semicon. Proc. 6 (2003) 193.
[18] C.R. Cho, N. Yarykin, R.A. Brown, O. Kononchuk, G.A. Rozgonyi, R.A. Zuhr, Appl. Phys. Lett. 74 (1999) 1263.
[19] V.N. Brudnyi, M.D. Vilisova, L.P. Porokhovnichenko, Russ. Phys. J 35 (1992) 939.
[20] P. Pellegrino, P. Leveque, J. Lalita, A. Hallen, C. Jagadish, B.G. Svensson, Phys. Rev. B 64 (2001), 195211.
[21] P.N.K. Deenaparanay, J.S. Williams, MRS Proceedings 540 (1998) 121.
[22] S. Limpijumnong, C.G Van de Walle, Phys. Rev. B 69 (2004), 035207.
[23] J.K.N. Lindner, Nucl. Instr. Meth. Phys. Res. B 127–128 (1997) 401.
[24] Y.S. Puzyrev, R.D. Schrimpf, D.M. Fleetwood, S.T. Pantelides, Appl. Phys. Lett. 106 (2015), 053505.
[25] Z.Q. Fang, D.C. Look, L. Polenta, J. Phys.: Condens. Matter 14 (2002) 13061.
[26] M. Horita, T. Narita, T. Kachi, J. Suda, Appl. Phys. Express 13 (2020), 071007.
[27] D. Haase, M. Schmid, W. Kürner, A. Dnen, V. Härle, F. Scholz, M. Buckard, H. Schweizer, Appl. Phys. Lett. 69, 2525 (1996).
[28] M. Mamor, V. Matias, A. Vantomme, A. Colder, P. Marie, P. Ruterana, Appl. Phys. Lett. 85 (2004) 2244.
[29] T.T. Duc, G. Pozina, N.T. Son, E. Janzen, T. Ohshima, C. Hemmingsson, Appl. Phys. Lett. 105 (2014), 102103.
[30] G. Alfieri, V.K. Sundaramoorthy, J. Appl. Phys. 126 (2019), 125301.